

Per-carrier nonlinear optical response of [111]-oriented piezoelectric InGaAs/GaAs multiple quantum wells

X. R. Huang, A. N. Cartwright, D. R. Harken, D. S. McCallum, and Arthur L. Smirl
Laboratory for Photonics and Quantum Electronics, 100 IATL, University of Iowa, Iowa City, Iowa 52242

J. L. Sánchez-Rojas, A. Sacedón, E. Calleja, and E. Muñoz
Departamento de la Ingeniería Electrónica, ETSI Telecomunicación, Universidad Politécnica de Madrid, Ciudad Universitaria, 28040-Madrid, Spain

(Received 12 April 1995; accepted for publication 13 September 1995)

We measure the per-carrier nonlinear responses caused by photoexcited carriers in two strained [111]-oriented InGaAs/GaAs multiple-quantum-well structures, and we compare them to that measured in a [100]-oriented structure. Without an external bias, we find that the absorption coefficient changes per photogenerated carrier for the [111]-oriented piezoelectric materials are smaller than for the [100]-oriented materials, not larger, as originally suggested. Subsequently, measurements of the per-carrier nonlinear responses as a function of reverse bias voltage demonstrate that the smaller per-carrier nonlinearities measured for the [111] structures are partially the result of a broadening of the excitons by the huge in-well fields, but can be primarily attributed to the quality of the [111]-grown materials. When corrected for differing in-well fields and for differing excitonic linewidths, the per-carrier responses are similar in magnitude, suggesting that the [111] response may eventually approach that of [100] material, but probably will not significantly exceed it. © 1996 American Institute of Physics. [S0021-8979(96)02501-9]

I. INTRODUCTION

A number of semiconductor optical and electro-optical devices (e.g., optical switching and logic devices) require a large nonlinear change of their optical properties (either absorptive or refractive) per absorbed photon or per injected carrier pair. The change in refractive index or absorption produced by a laser pulse is proportional to the shorter of either the pulse duration or the excited carrier lifetime. Optimally, the pulse duration and carrier lifetime are matched, in which case the switching energy (product of power and time) is determined primarily by the change in absorption coefficient per photogenerated (or injected) carrier pair. Therefore, any mechanism that has the potential to enhance the per carrier nonlinear response is of considerable interest. It has been suggested¹ that the screening of the huge piezoelectric fields present in strained-layer multiple-quantum-well (MQW) structures grown along the $\langle 111 \rangle$ and $\langle 211 \rangle$ directions might provide such an enhancement. The presence of the piezoelectric field along the growth direction in such materials shifts the exciton to the red through the quantum-confined Stark effect (QCSE). The nonlinearity then arises as the photogenerated (or injected) charge screens the piezoelectric field causing the exciton to shift to the blue as the QCSE is reduced.

Early theoretical work^{1,2} (based on mechanically free lattices) predicted a large nonlinear response for strained materials oriented in the $\langle 211 \rangle$ and $\langle 111 \rangle$ directions because of the screening of the strain-induced piezoelectric fields by photoexcited carriers that remain in the quantum wells (in-well screening). To date, however, there have been only a few measurements³⁻⁶ of the nonlinear response of these piezoelectric quantum wells. In the first measurement,³ the accumulated absorption change of a [211]-oriented InGaAs/GaAs MQW under cw excitation was shown to be an order of

magnitude larger than that measured in a similar structure grown in the [100] direction (which had no piezoelectric field along the growth direction). In addition, measurements³ of the photoluminescence following excitation of large carrier densities indicated that each sample initially recovered on a nanosecond time scale. Under the presumption of similar recombination lifetimes for the two samples, these initial results seemed to imply a factor of 10 enhancement of the per-carrier nonlinearities in the piezoelectric MQWs.

A subsequent comparison⁴ of [111]- and [100]-oriented strained MQWs using 1 ps excitation pulses confirmed that the steady-state nonlinearities were larger in the [111]-oriented piezoelectric sample than in the nonpiezoelectric [100]-oriented sample, but attributed the enhanced response to a carrier accumulation over the much longer lifetime measured for the [111] sample compared to the [100] sample—not to a larger per-carrier response. The much longer lifetimes⁴ measured for the [111] sample were attributed to the mechanically clamped lattice of the InGaAs/GaAs grown on GaAs. In such structures, the lattice constant of the substrate (GaAs) is imposed on the entire MQW. Therefore, the strain and the piezoelectric field are localized in the well and, as a result, a potential accumulates across the MQW region as shown schematically in Fig. 1. In such a structure, once the electrons and holes have escaped the wells and moved in opposite directions to the edges of the sample, they are separated in space by a potential that can approach that of the band gap. Under these circumstances, the recombination is nonexponential and extremely slow. In fact, in the previous studies by Cartwright *et al.*⁴ the sample recovered very little in the 1 μ s between laser pulses at low pump fluences. Until recently this extremely slow sample recovery precluded any temporal resolution of the optical nonlinearity and determination of carrier dynamics in piezoelectric MQWs.

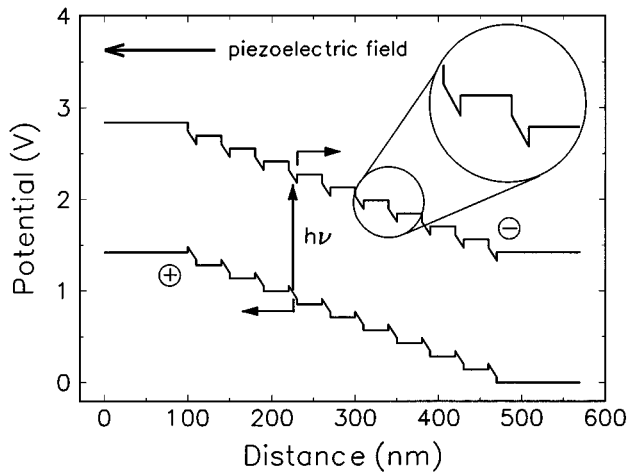


FIG. 1. Schematic of the mechanically clamped spatial band structure and motion of photogenerated carriers in a strained [111]-oriented multiple-quantum-well structure.

Recently, however, by embedding a piezoelectric MQW in a p - i - n structure specifically designed to reduce the lifetime of photoexcited carriers and by operating our laser system at a low repetition rate (25 kHz), we were able^{5,6} to isolate the nonlinear effects associated with the carriers injected by a single laser pulse from the cumulative effects of previous pulses. By doing this, we were able to temporally resolve the piezoelectric optical nonlinearities and to show that, for times long compared to the carrier escape time, the nonlinearities are dominated by long-range (out-of-well) screening of the piezoelectric field by carriers that have escaped the wells and moved to the edges of the MQW region; however, these measurements were not performed under conditions that were appropriate for extracting a per-carrier nonlinear figure of merit.

In this article we extend this work to provide the first measurements of the per-carrier nonlinear optical response associated with out-of-well screening of the piezoelectric field in strained, [111]-oriented InGaAs/GaAs p - i (MQW)- n structures. We have measured this per-carrier nonlinear response in two piezoelectric structures with dramatically different bandstructures and nonlinear responses, and we have compared it to that measured in a conventional nonpiezoelectric p - i (MQW)- n structure grown in the [100] direction. The per-carrier responses were first measured on the samples as grown (i.e., without any applied bias). The measurements were then repeated as a function of reverse bias. By so doing, we were able to measure the per-carrier nonlinear response of each sample at comparable in-well fields and to eliminate field-induced broadening from the comparison.

II. SAMPLES STUDIED

The two piezoelectric samples studied here are the same two p - i (MQW)- n structures that were used in our recent work.^{5,6} Specifically, in the first of these (no. 279), the MQW region consists of ten 10-nm-wide In_{0.15}Ga_{0.85}As/GaAs wells separated by 15-nm-wide GaAs barriers. The MQW region is

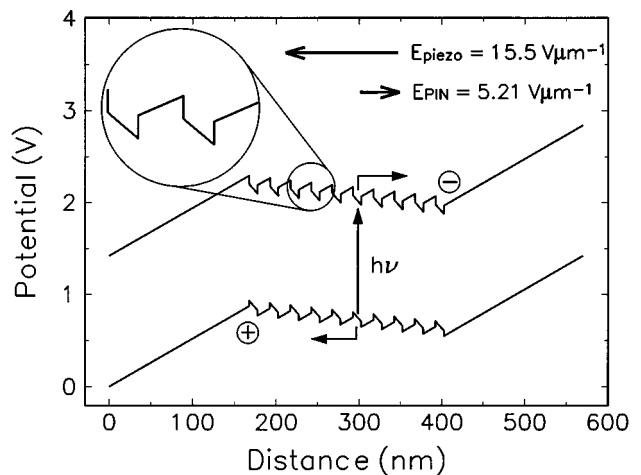


FIG. 2. Schematic of the spatial band structure and motion of photogenerated carriers in the [111]-oriented InGaAs/GaAs p - i (MQW)- n sample no. 279.

clad by 117.5-nm-wide undoped GaAs spacer layers. The sample was grown on an n^+ -doped [111]-oriented substrate, and capped by a 300-nm-thick layer of p^+ GaAs. The concentration of both n and p dopants is $>2 \times 10^{18} \text{ cm}^{-3}$, which is more than sufficient to allow a built-in potential of $\sim 1.4 \text{ V}$ to develop between the doped regions when the sample is not externally biased.

The spatial band structure of sample 279 (without external bias) is shown in Fig. 2 for convenience. The procedure used to calculate that band structure^{5,7} and the piezoelectric constants^{8,9} used in that calculation are discussed in some detail elsewhere. The piezoelectric field in the QWs ($\sim 155 \text{ kV/cm}$) is arranged to be in opposition to the p - i - n electric field ($\sim 52.1 \text{ kV/cm}$), and, therefore, the total in-well field (the difference between the piezoelectric field and the p - i - n field) is about 100 kV/cm , equivalent to the piezoelectric field in a strained, undoped In_{0.1}Ga_{0.9}As/GaAs MQW.

The thickness of the well and the barrier layers were carefully chosen so that the accumulated decrease in potential over the MQW region due to the piezoelectric field is greater than the accumulated increase due to the p - i - n field. Consequently there are local potential minima for electrons and holes at opposite ends of the MQW region. As we have recently demonstrated,⁵ at low excitation levels in an unbiased sample, electrons and holes that are photogenerated in the QWs will escape and move to these minima to produce a space-charge field that is in opposition to the piezoelectric field. As a result, the total field in the QW will be reduced, and the exciton will shift to the blue because of a reduction in the QCSE.

We have also shown⁶ that, as the excitation levels are increased, the field in the QWs (as indicated by this blue shift) saturates. This saturation demonstrates that the sample cannot be optically driven (in the absence of an external potential) beyond flatband conditions in the QW region. Any attempt to optically produce a positive cumulative potential across the MQW region in this sample by producing more carriers than is needed to flatten the average potential will produce movement of charge (i.e., a current) so as to screen

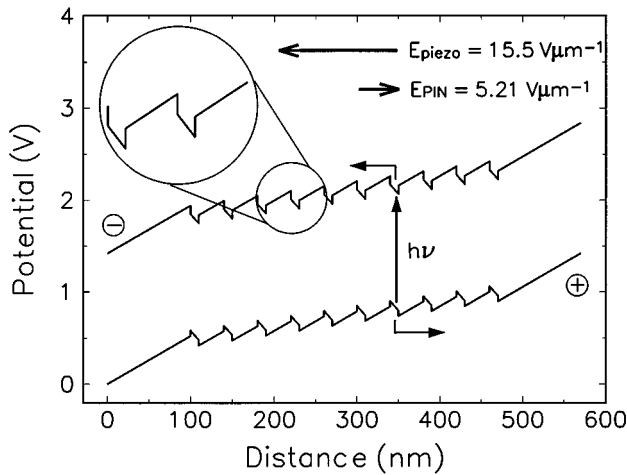


FIG. 3. Schematic of the spatial band structure and motion of photogenerated carriers in the [111]-oriented InGaAs/GaAs p - i -(MQW)- n sample no. 280.

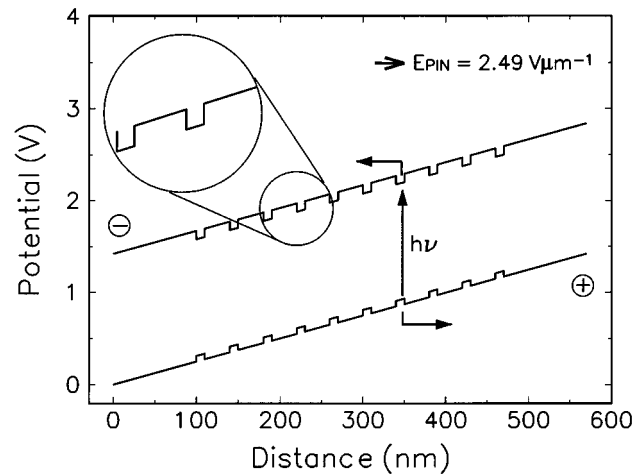


FIG. 4. Schematic of the spatial band structure and motion of photogenerated carriers in the [100]-oriented InGaAs/GaAs p - i -(MQW)- n .

the p - i - n field. This screening of the p - i - n field will allow an increase of the net in-well field. The increase in the in-well field will, in turn, tend to tilt the cumulative potential back toward having a local minima, thus producing a current that opposes the change. The quasisteady state between these two currents ensures that the bands cannot be driven beyond having an average potential that is flat across the MQW region. If the latter were not so, then the blue shift would become a red shift at higher excitation levels, and it does not. This behavior is of interest, but it is of no consequence to us here, since we perform all of our per-carrier measurements in a regime where the change in potential due to screening is small compared to the unscreened potential difference between the two minima.

As a final point on this sample, we note that the potential difference between these two minima is ~ 0.3 V which is much smaller than the potential difference of ~ 1.4 V between the ends of the undoped piezoelectric MQW structures used in earlier attempts⁴ to measure the nonlinear response. Consequently, the recombination lifetime of the spatially separated electrons and holes will be greatly reduced compared to those earlier structures.

The second piezoelectric sample (no. 280) is identical to the first except that the barriers have a thickness of 30 nm. This seemingly minor change in sample design causes a major change in the spatial band structure, as illustrated in Fig. 3. As with sample no. 279, the piezoelectric field in the QWs (~ 155 kV/cm) is in opposition to the p - i - n electric field (~ 52.1 kV/cm), and the total in-well field is about 100 kV/cm. In contrast to no. 279, however, the thicknesses of the well and the barrier layers dictate that the accumulated decrease in potential over the MQW region due to the piezoelectric field is smaller than the accumulated increase due to the p - i - n field. Consequently there are no local potential minima for electrons and holes at opposite ends of the MQW region for sample no. 280. In this case (as we have also recently demonstrated⁵), when electrons and holes are photogenerated in the QWs, they will escape and move (in the

opposite direction to the carriers in no. 279) to the doped regions to produce a space-charge field that reinforces the piezoelectric field. As a result, the total field in the QWs will be increased, and the exciton will shift to the red because of an increase in the QCSE. At higher excitation levels the screening of the in-well field can never become large enough to produce a negative slope in the average potential (and a corresponding blue shift). That is, as with sample no. 279 and for similar reasons, sample no. 280 cannot be optically driven beyond having an average potential that is flat across the MQW region.

The third sample is identical to sample no. 280 except that it was grown in the [100] direction. For completeness, the spatial band structure of the nonpiezoelectric sample is shown in Fig. 4. In the absence of an external bias, the only field in the QWs is the built-in p - i - n field (~ 25 kV/cm), which is smaller than the net in-well field in the other two samples. In this sample, photogenerated carriers will escape the wells and move to screen p - i - n field causing a blue shift of the exciton as the QCSE is reduced.

As a final comment on these three samples, we note that the 10-nm-wide InGaAs well thicknesses used here are below¹⁰ the critical thicknesses for both the $\langle 100 \rangle$ and $\langle 111 \rangle$ orientations for an In mole fraction of 0.15. Consequently, we would not expect misfit dislocations to significantly reduce the strain-induced field and, thereby, to reduce the associated nonlinear response. Nevertheless, we checked for dislocations in three ways. First, we used a microscope to visually inspect each sample, and we observed no evidence of dislocation formation. Second, we performed x-ray-diffraction studies on similar samples (with $x=0.15$) that revealed no evidence of dislocation formation. Finally (and most importantly), we measured the excitonic shifts that correspond to optically induced flatband conditions, and we measured the shift of the exciton as a function of externally applied electrical reverse bias. A comparison of these two sets of measurements, using the procedure described in Ref. 5, demonstrated quantitative agreement with the spatial band

structures calculated (and shown qualitatively in Figs. 2–4) assuming no dislocation formation.

III. MEASUREMENT OF THE [111] PER-CARRIER NONLINEAR RESPONSE

In both the piezoelectric and nonpiezo p - i (MQW)- n structures studied here, the change in absorption coefficient $\Delta\alpha$ is caused by the screening of the perpendicular in-well field E_{\perp} (intrinsic, built in, or applied) by a photogenerated space charge field E_{sc} ,

$$\Delta\alpha(\lambda) = \alpha(E_{\perp} - E_{sc}) - \alpha(E_{\perp}). \quad (1)$$

We have shown elsewhere¹¹ that, when this quantity is measured under a restricted set of conditions, the normalized spectrum $\Delta\alpha(\lambda)/N$ (obtained by dividing the change in absorption coefficient by the density of photogenerated carriers N) will have a shape and an amplitude that are independent of excitation level, but that the spectrum will shift slightly and linearly with excitation level. Except for this shift, these are exactly the properties that allow the definition of a per-carrier absorptive cross section for bleaching nonlinearities. The latter has been commonly used to quantify the effectiveness of optically created carriers in changing the absorption coefficient.^{12–17} For this reason we choose to use the peak change in absorption coefficient per carrier,

$$\sigma_{eh} = \frac{\Delta\alpha(\lambda_{peak})}{N}, \quad (2)$$

as the measure of the strength of the nonlinearity, where λ_{peak} designates the wavelength at which $\Delta\alpha$ is a maximum. For the samples used here (each of which contains ten 10-nm-thick wells), the density of carriers N generated in each well is uniform from the front to the back of the sample to within 10%, and the magnitude of the average carrier density N is known to within $\pm 15\%$.

The conditions necessary for σ_{eh} to be a constant and independent of excitation density are:¹¹

- (i) that the number of carriers that escape the wells and move to screen the field increases linearly with fluence and with photoexcited carrier density;
- (ii) that the resulting photogenerated space-charge field E_{sc} must be small compared to the initial unexcited in-well perpendicular field E_{\perp} ;
- (iii) that the area under the excitonic absorption line must remain approximately constant (i.e., bleaching is negligible); and
- (iv) that the shift in the center wavelength of the excitonic peak caused by photoexcitation, $\Delta\lambda(E_{\perp} - E_{sc}) - \Delta\lambda(E_{\perp})$, is small compared to the excitonic linewidth Γ_0 .

All of our measurements were performed well within this “linear” regime.

Also, we have established¹¹ that (in the low-excitation regime where σ_{eh} can be defined) σ_{eh} follows the following phenomenological scaling expression:

$$\sigma_{eh} = \pm \left(f \frac{eCN_w I_w}{\epsilon} \right) \frac{\alpha_0}{\Gamma_0} \left. \frac{\partial \Delta\lambda(E)}{\partial E} \right|_{E_{\perp}}, \quad (3)$$

where f is the fraction of the photogenerated carrier density that escapes the wells and moves to screen the perpendicular field, e is the fundamental charge, C is a constant that is determined by whether the excitonic lineshape is Gaussian or Lorentzian, ϵ is the dielectric constant of the material, α_0 is the amplitude, and Γ_0 is the half-width at half-maximum linewidth of the exciton. Finally, $\Delta\lambda(E)$ gives the shift of the center wavelength of the exciton with in-well field. In agreement with previous studies,^{11,18–21} we found that the excitonic peak in our samples shifted quadratically with the perpendicular field [$\Delta\lambda(E_{\perp}) = \gamma E_{\perp}^2$] for in-well fields below ~ 40 kV/cm. Above this value, the excitonic shift continued to increase with the field, but the shift was no longer quadratic.¹¹ For the three samples considered here the number of wells and the well widths are identical. Consequently, the first term (in parenthesis) in Eq. (3) would be expected to be constant.

We emphasize that the scaling of the per-carrier Stark-shifted nonlinearity σ_{eh} with well number, electric field, amplitude, and width of the excitonic transition [as given by Eq. (3)] has been demonstrated¹¹ by measuring the per-carrier nonlinear response of a number of MQW structures as a function of temperature, bias, and materials system.

For our studies, values for σ_{eh} were extracted from standard two-color pump-probe differential transmission measurements. These measurements were performed using two independently tunable, cavity dumped, cw-mode-locked dye lasers. Each laser produced pulses of ~ 2 ps in duration (full width at half-maximum intensity), and the measured jitter between pulses from the two lasers was always less than 10 ps. One laser was used to generate a known density of carriers N by tuning it to a fixed wavelength slightly to blue of the heavy-hole exciton, while the other was used as a variable wavelength probe and was tuned across the excitonic absorption profile. The focused spot size of the probe at the sample was adjusted to be 1/3 of the pump spot size (100 μm , half-width at e^{-1} of the maximum) to ensure relatively constant excitation over the probe spot.

All measurements reported here were performed with a fixed time delay of 800 ps between the pump and probe pulses. This delay was chosen because a separate study of the photoexcited carrier dynamics⁶ showed that the photoexcited carriers had completely escaped the wells by this time, but had not yet undergone significant recombination. In addition, separate in-plane transport measurements were performed using standard techniques^{22,23} to determine the loss of carriers by diffusion out of the optically excited region. All estimates of optically created carrier densities reported here take this diffusion into account. The laser repetition rates (25 kHz for sample 279 and 147 kHz for the other two samples) were chosen to ensure an acceptable signal-to-noise ratio yet to allow almost complete recovery of the samples.

Under these conditions, standard lock-in techniques were used to measure the difference ΔT in the probe-pulse transmission with and without the pump present as a function of wavelength and fluence. The differential absorption spectrum was then extracted for each fluence F and time delay τ using the expression

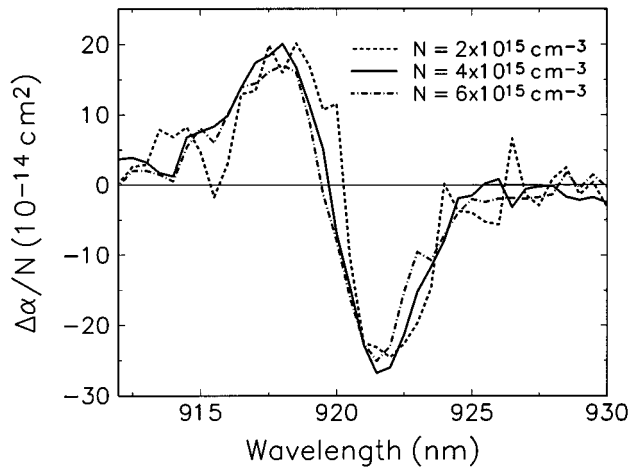


FIG. 5. Stark-shifted absorption change per photogenerated carrier as a function of wavelength for the [111]-oriented sample no. 279 for selected injected carrier densities at 80 K.

$$\Delta\alpha(\lambda, \tau=800 \text{ ps}, F) = -\frac{1}{N_w l_w} \left[\ln\left(1 + \frac{\Delta T}{T}\right) \right], \quad (4)$$

where $N_w l_w$ is the total thickness of quantum well material. All measurements were performed at 80 K to improve the signal-to-noise ratio. Most important, we emphasize that values for σ_{eh} were only extracted from regimes where these spectra were clearly shown to be independent of excitation fluence F .

IV. PER-CARRIER RESPONSE OF UNBIASED SAMPLES

We measured $\Delta\alpha/N$ for each of the three samples described in Sec. II as grown (i.e., without an externally applied bias). First, however, we measured the peak $\Delta\alpha$ as a function of fluence for each sample to ensure that the amplitude of the Stark shift varied linearly with fluence over the range used to extract σ_{eh} . Operation within this regime, in turn, ensured that $E_{\text{sc}} \ll E_{\perp}$. In addition, we verified that the shifts in the center wavelength of the exciton, $\Delta\lambda(E_{\perp} - E_{\text{sc}}) - \Delta\lambda(E_{\perp})$, were less than one-tenth that of the excitonic linewidth $\Gamma_0(E_{\perp})$ for all measurements reported here.

Results of such measurements on sample no. 279 (see Fig. 2) are shown in Fig. 5 for selected excitation levels. The quantity actually plotted in Fig. 5 (and in similar figures throughout) is

$$[\Delta\alpha(\lambda, 800 \text{ ps}, F) - \Delta\alpha(\lambda, -50 \text{ ps}, F)]/N$$

for the in-well carrier densities indicated and for a sample temperature of 80 K. We subtracted the spectrum at -50 ps (i.e., $\sim +40 \mu\text{s}$) to ensure that we compensated for any residual background that accumulated from pulse to pulse. From Fig. 5 it is clear that the exciton shifts to the blue with increasing fluence, consistent with the band structure shown in Fig. 2. It is also clear that for carrier densities within this regime that the shape and magnitude of the quantity $\Delta\alpha(\lambda)/N$ is independent of excitation level. Under these conditions,

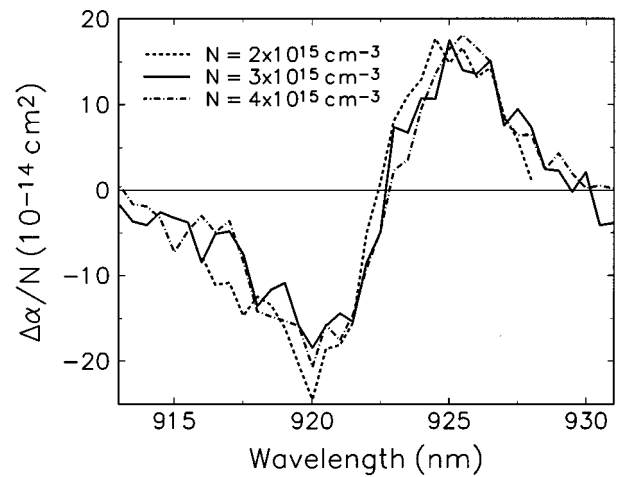


FIG. 6. Stark-shifted absorption change per photogenerated carrier as a function of wavelength for the [111]-oriented sample no. 280 for selected injected carrier densities at 80 K.

the peak change in the absorption coefficient per carrier, $\sigma_{\text{eh}} \equiv \Delta\alpha_{\text{peak}}/N$, can be taken as a valid per-carrier figure of merit. The value extracted from Fig. 5 for the [111]-oriented sample no. 279 and 80 K is $\sigma_{\text{eh}} = (27 \pm 7) \times 10^{-14} \text{ cm}^2$. Similar data are presented in Fig. 6 for sample no. 280. In contrast to no. 279, notice that the spectra for no. 280 are indicative of a red shift of the exciton, consistent with the band structure shown in Fig. 3, and that $\sigma_{\text{eh}} = (21 \pm 6) \times 10^{-14} \text{ cm}^2$. Finally, data for the [100]-oriented samples are presented in Fig. 7. The spectra are indicative of a blue shift and $\sigma_{\text{eh}} = (480 \pm 100) \times 10^{-14} \text{ cm}^2$.

In view of the scaling law given by Eq. (3), the measured values for σ_{eh} given in the previous paragraph, at first, appear surprising. All other parameters being equal (namely, α_0 and Γ_0), inspection of Eq. (3) would suggest that σ_{eh} should increase with in-well electric-field strength. Consequently, since the in-well field in each of the [111]-oriented samples is $\sim 100 \text{ kV/cm}$, and it is $\sim 25 \text{ kV/cm}$ for the [100]

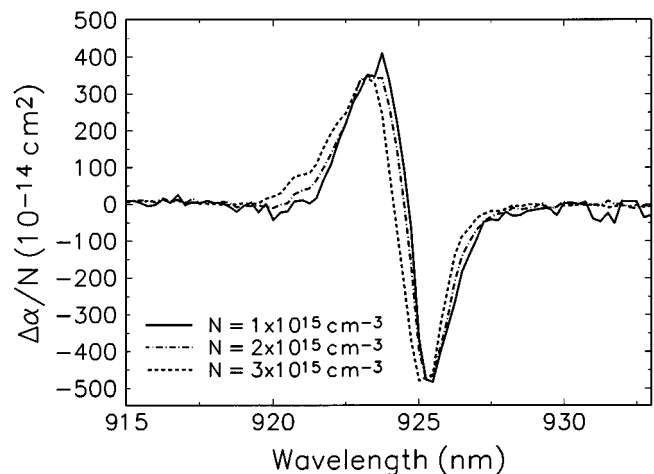


FIG. 7. Stark-shifted absorption change per photogenerated carrier as a function of wavelength for the [100]-oriented sample for selected injected carrier densities at 80 K.

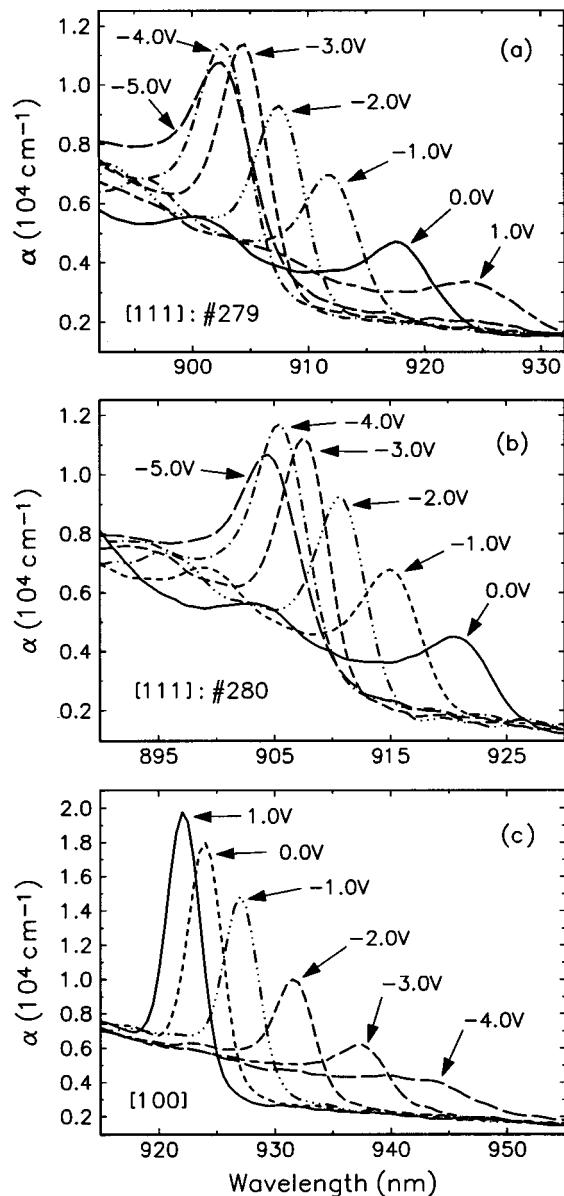


FIG. 8. Linear absorption spectra at 80 K as a function of reverse bias for the [111]-oriented samples (a) no. 279 and (b) no. 280, and (c) for the [100]-oriented sample.

sample, one might expect from the field dependence alone that the σ_{eh} for the [111] samples would be equal, but larger than for the [100] sample. Indeed, we find that σ_{eh} for no. 279 is roughly equal to σ_{eh} for no. 280, but surprisingly that σ_{eh} for the [100] sample is a factor of 20 larger than for no. 279 or no. 280. The implication is that the exciton is broadened substantially in the [111] samples compared to the [100] sample. Indeed, the excitonic linewidths for the unbiased samples at 80 K are separately measured to be 3.4, 4.7, and 1.1 nm for the [111]-oriented samples 279 and 280 and for the [100]-oriented sample, respectively. The question then arises as to whether this broadening of the excitonic linewidths and the associated smaller per-carrier nonlinearities measured in the piezoelectric samples are the result of broadening by the huge in-well fields, whether they can be

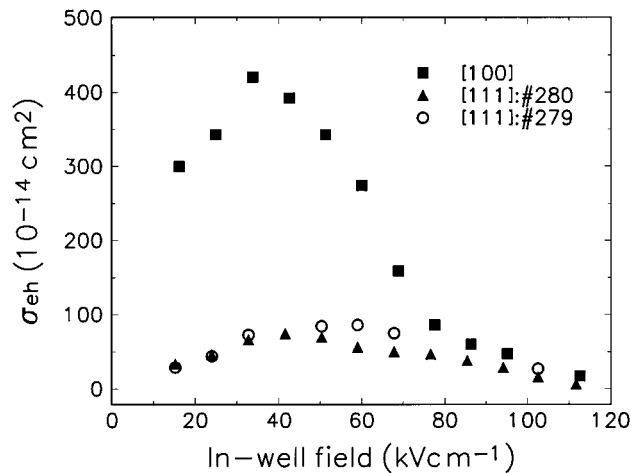


FIG. 9. Comparison of the per-carrier nonlinear response σ_{eh} of the [111]-oriented samples no. 279 (open diamonds) and no. 280 (solid circles) and the [100]-oriented sample (solid squares) as a function of in-well field at a temperature of 80 K.

attributed to material quality, or whether they are the result of some intrinsic difference in the nonlinear mechanisms. In the following section, in order to address this issue, we perform the first side-by-side comparison of the strained [111]- and [100]-oriented MQWs as a function of bias voltage. By so doing we are able to measure the per-carrier nonlinear response of each sample at comparable in-well fields and to eliminate field-induced broadening from the comparison.

V. PER-CARRIER RESPONSE AS A FUNCTION OF BIAS VOLTAGE

The shifts in the excitonic peaks with applied voltage for each of the samples used here are shown in Fig. 8. Notice that the peak shifts to the blue with increasing reverse voltage for the [111]-oriented sample no. 279 and for sample no. 280 and to the red for the [100]-oriented sample, as expected for the band structures shown in Figs. 2, 3, and 4, respectively. The per-carrier response σ_{eh} was measured at each reverse bias voltage for each sample, always taking care to ensure that we were operating in the regime where σ_{eh} can be defined, as described in Sec. III. In particular, we emphasize that, in determining σ_{eh} for each bias voltage, the photoinduced shift in the excitonic peak was always less than 0.1 of the excitonic linewidth. Also, for each bias voltage and each sample, the in-well field was calculated using the same procedure^{5,7-9} used to calculate the band structures shown in Figs. 2-4.

The σ_{eh} measured for each sample are plotted as a function of net in-well field in Fig. 9. Several features are worth noting. First, notice that σ_{eh} for the [100]-oriented MQW is much larger than those for the [111] samples for modest, but equal, in-well fields. This feature suggests that the remaining difference in the σ_{eh} for the two samples can be attributed directly to the “intrinsically” broader exciton in the [111] samples (which may be an indication of material quality). Next, notice that the general trends are similar for each sample. Specifically, for small in-well fields, σ_{eh} increases

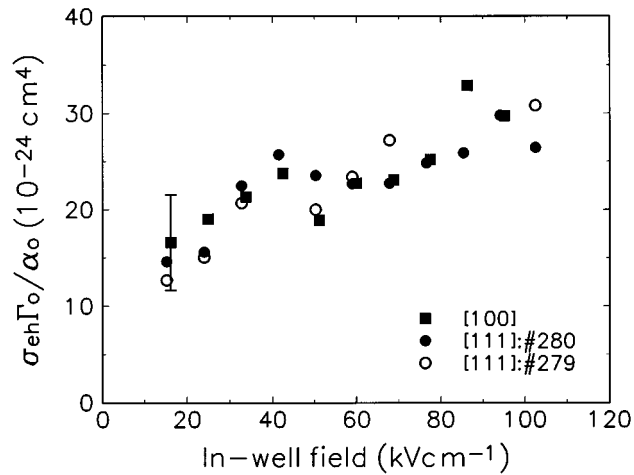


FIG. 10. Comparison of the normalized per-carrier nonlinear response, $\sigma_{eh}\Gamma_0/\alpha_0$, of the [111]-oriented samples no. 279 (open diamonds) and no. 280 (solid circles), and the [100]-oriented sample (solid squares) as a function of in-well field at a temperature of 80 K.

with the field, consistent with negligible broadening of the exciton with field and with an increasing (quadratic) shift of the exciton with field [see Eq. (3)]. At higher in-well fields, σ_{eh} decreases with increasing in-well field, consistent the onset of field-induced broadening of the exciton. Finally, notice that at the highest in-well fields, when field-induced broadening is expected to dominate, the σ_{eh} for all three samples become roughly equal (within a factor of 2).

These tendencies are made clearer if we plot the normalized quantity $\sigma_{eh}\Gamma/\alpha_0$ to remove the effect of excitonic broadening, as we have done in Fig. 10. Notice that the quantity $\sigma_{eh}\Gamma/\alpha_0$ is roughly the same for each sample. Since the oscillator strength (as represented by the area under the excitonic peak) is approximately the same for each sample and since the in-well fields are equal, this result further substantiates that the smaller σ_{eh} obtained for the [111]-oriented samples (shown in Fig. 9) are mainly associated with the larger excitonic linewidths (and smaller amplitudes) in the [111] samples and that this larger linewidth is most probably related to less than optimized material quality or to some fundamental limitation of growth in the [111] direction.

VI. CONCLUSIONS

Consequently, we conclude from these measurements that the per-carrier nonlinear optical response of piezoelectric MQWs can be optimized by properly adjusting the net in-well fields. We also conclude that we might expect further improvement (perhaps as much as a factor of 6) in the per-carrier nonlinear optical response of piezoelectric MQWs with optimized growth conditions, but that the per carrier

nonlinearities will probably not exceed those of [100] materials. Nevertheless, these materials are likely to continue to gain attention because of the additional design flexibility that the in-well piezoelectric fields provide. For example, in [111] structures, because of the presence of the in-well piezoelectric field (which can be arranged to oppose the p - i - n field), it is always possible to engineer the bandstructure to provide the optimal in-well bias conditions without an externally applied bias, while this is not possible in [100] structures without severely restricting the width of the intrinsic region.

ACKNOWLEDGMENTS

The work at the University of Iowa was supported in part by the Office of Naval Research, the National Science Foundation, and the Advanced Research Projects Agency, and the work at the Universidad Politécnica de Madrid by CICYT Projects No. TIC93-0025 and No. TIC 93-0026. The work at both institutions was jointly supported by a Collaborative Research Grant from NATO.

- ¹D. L. Smith and C. Mailhot, Phys. Rev. Lett. **58**, 1246 (1987).
- ²D. L. Smith and C. Mailhot, J. Vac. Sci. Technol. A **5**, 2060 (1987).
- ³I. Sela, D. E. Watkins, B. K. Laurich, D. L. Smith, S. Subbanna, and H. Kroemer, Appl. Phys. Lett. **58**, 684 (1991).
- ⁴A. N. Cartwright, D. S. McCallum, T. F. Boggess, A. L. Smirl, T. S. Moise, L. J. Guido, R. C. Barker, and B. S. Wherrett, J. Appl. Phys. **73**, 7767 (1993).
- ⁵X. R. Huang, D. R. Harken, A. N. Cartwright, D. S. McCallum, A. L. Smirl, J. L. Sánchez-Rojas, A. Sacedón, F. González-Sanz, E. Calleja, and E. Muñoz, J. Appl. Phys. **76**, 7870 (1994).
- ⁶D. R. Harken, X. R. Huang, D. S. McCallum, A. L. Smirl, J. L. Sánchez-Rojas, A. Sacedón, E. Calleja, and E. Muñoz, Appl. Phys. Lett. **66**, 857 (1995).
- ⁷J. L. Sánchez-Rojas, A. Sacedón, F. Calle, E. Calleja, and E. Muñoz, Appl. Phys. Lett. **65**, 2214 (1994).
- ⁸R. A. Hogg, T. A. Fisher, A. R. K. Willcox, D. M. Whittaker, M. S. Skolnick, D. J. Mowbray, J. P. R. David, A. S. Pabla, G. J. Rees, R. Grey, J. Woodhead, and J. L. Sánchez-Rojas, Phys. Rev. B **48**, 8491 (1993).
- ⁹R. L. Tober and T. B. Bahder, Appl. Phys. Lett. **63**, 2369 (1993).
- ¹⁰T. Anan, K. Nishi, and S. Sugou, Appl. Phys. Lett. **60**, 3159 (1992).
- ¹¹A. N. Cartwright, X. R. Huang, and Arthur L. Smirl, IEEE J. Quantum Electron. **31**, 1726 (1995).
- ¹²D. S. Chemla, D. A. B. Miller, P. W. Smith, A. C. Gossard, and W. Wiegmann, IEEE J. Quantum Electron. **QE-20**, 265 (1984).
- ¹³D. S. Chemla, D. A. B. Miller, and P. W. Smith, Opt. Eng. **24**, 556 (1985).
- ¹⁴D. S. Chemla and D. A. B. Miller, J. Opt. Soc. Am. B **2**, 1155 (1985).
- ¹⁵K. Tai, J. Hegarty, and W. T. Tsang, Appl. Phys. Lett. **51**, 86 (1987).
- ¹⁶A. Miller, R. J. Manning, P. K. Milsom, D. C. Hutchings, D. W. Crust, and K. Woodbridge, J. Opt. Soc. Am. B **6**, 567 (1989).
- ¹⁷S. Schmitt-Rink, D. S. Chemla, and D. A. B. Miller, Adv. Phys. **38**, 2 (1989).
- ¹⁸G. Lengyel, K. W. Jelley, and R. W. H. Engelmann, IEEE J. Quantum Electron. **QE-26**, 296 (1990).
- ¹⁹C. -H. Lin, J. M. Meese, and Y. -C. Chang, J. Appl. Phys. **75**, 2618 (1994).
- ²⁰D. A. B. Miller, J. S. Weiner, and D. S. Chemla, IEEE J. Quantum Electron. **QE-22**, 1816 (1986).
- ²¹W. Chen and T. G. Andersson, Semicond. Sci. Technol. **7**, 828 (1992).
- ²²G. Livescu, D. A. B. Miller, T. Sizer, D. J. Burrows, J. E. Cunningham, A. C. Gossard, and J. H. English, Appl. Phys. Lett. **54**, 748 (1989).
- ²³D. S. McCallum, A. N. Cartwright, X. R. Huang, T. F. Boggess, A. L. Smirl, and T. C. Hasenberg, J. Appl. Phys. **73**, 3860 (1993).